2011 IEEE International Conference on Robotics and Automation
Shanghai International Conference Center
May 9-13, 2011, Shanghai, China

Kinematic Optimization for Isotropic Stiffness of Redundantly Actuated Parallel Manipulators

Hyunpyo Shin, SungCheul Lee, Jay. I. Jeong, and Jongwon Kim

***Abstract*— A kinematic optimization procedure for redundantly actuated parallel manipulator is developed to ensure the isotropic antagonistic stiffness in a workspace. The kinematic parameters of the mechanism are optimized to maximize and equal out antagonistic stiffness of the redundantly actuated manipulator when size and shape of the usable workspace are given but position in the entire workspace is not. The proposed procedure is verified with a 2-DOF planar manipulator by experiments. The experimental results show that the proposed procedure is useful for designing the redundantly actuated parallel manipulator with isotropic antagonistic stiffness in a predefined usable workspace as a design constraint.**

***Index Terms*— Mechanism Design of Manipulators; Parallel Robots; Redundant Robots.**

I. Introduction

REDUNDANTLY actuated parallel manipulators (or over-actuated parallel manipulators) have many advantages such as enlarged dexterous workspace and higher stiffness compared to the non-redundant analogues. Kinematic singularity region inside the workspace can mostly be eliminated in redundant actuation and the workspace can be enlarged [1]. In addition, internal preload control can enhance the antagonistic stiffness of the mechanism [2,3,4,5].

In order to design the redundantly actuated parallel mechanism, the determination of kinematic parameters of the mechanism and number of excessive actuators, that is force redundancy, should be carefully considered in the kinematic design process.

In previous works, the kinematic parameter optimization of the workspace and stiffness for non-redundantly actuated parallel mechanisms has been examined. Liu and Wang [6] introduced performance indexes such as the global conditioning index, global velocity index, global payload index, and global stiffness index within the framework of the performance atlas of the 5-bar parallel manipulator. They proposed the maximal inscribed circle (MIC) for practical applications and the maximal inscribed workspace (MIW) to perform kinematic optimization [7]. Regarding workspace analysis and optimization, Kosinska *et al.* [8] designed a set of kinematic parameters of a 3-DOF spatial orientation manipulator using constraint equations to produce a specified workspace. Ceccarelli and Lanni [9] optimized a 3R serial manipulator that maximizes the workspace and minimizes the size of the manipulator within limit constraints of a predefined workspace. Carbone and Ceccarelli [10] also suggested indices for stiffness performance evaluation.

In cases of the redundantly actuated parallel mechanisms, Lee *et al*. [11] discussed isotropy of the stiffness and gradient of the isotropy in the optimization of a redundantly actuated 5-bar parallel manipulator. Although they considered antagonistic stiffness, the workspace and its shape were not included in the optimization procedure. Kurtz *et al.* [12] performed a uniformity of the dexterity and an actuator force optimization of a redundantly actuated parallel manipulator. Chakarov [13] discussed antagonistic stiffness of a parallel manipulator and he showed that the maximum compliance in a random direction could be reduced by controlling the internal preload of linear actuators.

The optimization process of antagonistic stiffness is not easy even though shape and size of the workspace is predefined as design constraint. In the optimization process, the various kinematic parameters are tested and one optimal parameter set is determined to maximize or equalize the antagonistic stiffness of the mechanism. The shape and size of the entire workspace, however, could be changed dramatically by small deviation of the kinematic parameters. This means that the position of the usable workspace should be rearranged as the change of the entire workspace. Moreover, the antagonistic stiffness of the mechanism must be recalculated with every candidate of kinematic parameters. Thus, the magnitude and isotropy of the antagonistic stiffness should be considered in design process of the mechanism as well as the workspace of the mechanism.

With an initial kinematic design, an optimization process for kinematic parameters and degrees of force redundancy usually follows. The magnitude of antagonistic stiffness needs to be maximized by adjusting the length of the linkages and position of joints. Moreover, isotropy of the antagonistic stiffness should be guaranteed especially for industrial implementation

This paper was supported by the second stage of the Brain Korea 21 Program of Seoul National University, by the Korean Ministry of Knowledge and Economy through a research project titled, “Development of multi-axis vibrational evaluation equipment.”

Hyunpyo Shin and Jongwon Kim are with School of Mechanical and Aerospace Engineering, Seoul National University, Sillim 9-Dong, Gwanak-Gu, Seoul, South Korea, 151-744 (e-mail: hpshin@snu.ac.kr jongkim@rodel.snu.ac.kr).

SungCheul Lee is with Korea Institute of Machinery and Materials, 104 Sinseongno, Yuseong-gu, Daejeon, South Korea, 305-343 (e-mail: sclee@kimm.re.kr).

Jay. I. Jeong is with School of Mechanical and Automotive Engineering, Kookmin University, 861-1 Jeongneung-Dong, Songbuk-Gu, Seoul, South Korea, 136-702 (corresponding Author to provide phone: +82-2-910-4419; fax: +82-2-910-4839; e-mail: jayjeong@kookmin.ac.kr).

of the redundantly actuated parallel mechanism. In designing the parallel mechanism for machine tools and positioning stages for examples, the antagonistic stiffness better be uniform with respect to any direction of external forces [14, 15].

The usable workspace shape for the parallel manipulator is supposed to be rectangles, hexahedrons, circles, and cylinders because of practical use [16]. Thus, it is reasonable to consider the workspace shape as a constraint for the kinematic design procedure. Consequently, the kinematic parameters should be optimized to maximize the magnitude and to ensure the isotropy of the stiffness with the shape and size of the workspace given.

This study presents a novel optimization procedure and experimental verification to maximize the magnitude of antagonistic stiffness and to ensure the isotropy of the antagonistic stiffness in a predefined usable workspace. In the predefined workspace, the several checkpoints are selected in order to check the magnitude and isotropy of the stiffness. The stiffness index was formulated by using the stiffness matrix of the given mechanism since the magnitude of stiffness is related to the determinant of the stiffness matrix. The isotropy of the stiffness is related to the inverse of a condition number of the stiffness matrix. As validation of the proposed optimization procedure, the experiment on the optimization result of the 2-DOF parallel manipulator is conducted to verify the validity of the stiffness analysis and the performance improvement achieved by the method.

This paper is organized as follows. In Section 2, the proposed optimization method is introduced. An optimization index is formulated based on the antagonistic stiffness modeling in Section 3. Optimization and its experiment about the 2-DOF planar parallel manipulator are suggested in Section 4. Finally, some concluding remarks are presented in Section 5.

II. Optimization Method

In this study, a concept called an isotropic antagonistic stiffness workspace (ISW) is introduced. The ISW should guarantee several conditions. First, there is no kinematic singularity in ISW. Second, there is no stiffness singularity in ISW. Third, the antagonistic stiffness in the workspace is isotropic and maximized. Fourth, the shape of workspace is simple such as a rectangle, circle, or triangle shown in Fig.1. [7,17,18]. By ensuring ISW for the given mechanism, the workspace and antagonistic stiffness is guaranteed to be isotropic and maximized in a given workspace.

In general, the workspace optimization can be accomplished as a result of an exhaustive search of all kinematic parameters for which the solution of inverse kinematics exists. The workspace calculation that accounts for every combination of the kinematic parameters is very cost-demanding and is not appropriate to secure predefined shape of a usable workspace. Therefore, a goal-oriented optimization procedure maximizing performance index for predefined workspace shape is required.

As for related studies, Lee *et al.* [19] defined five spatial positions and orientations. Then they calculated the dimensions of the geometric parameters (DH parameter) of the 3-R manipulator so that the manipulator places its end-effector at

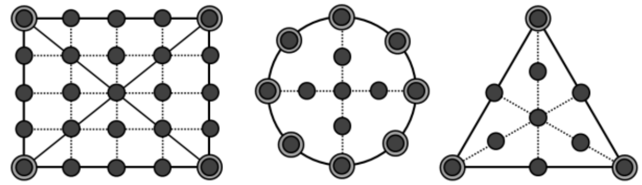

Fig. 1. Examples of isotropic antagonistic stiffness workspaces and their check points

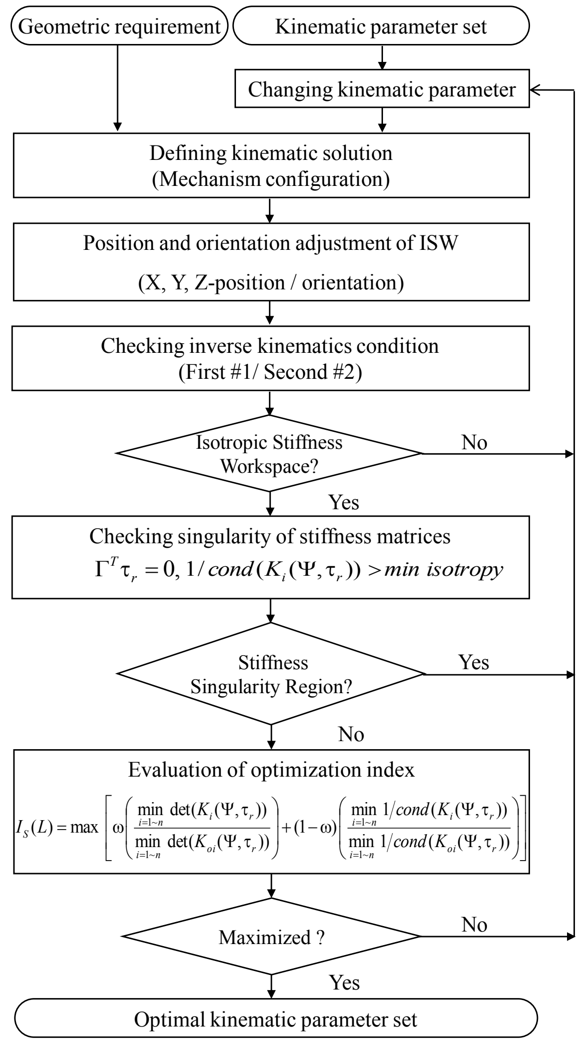

Fig. 2. Optimization procedure with consideration of workspace and antagonistic stiffness

these predefined locations. Morgan and Wampler [20] performed kinematic parameter optimization of a 4-bar parallel manipulator so that the manipulator would be able to follow a predefined path. They optimized the manipulators in geometric aspect at each predefined checkpoint. Stocco *et al.* [21] showed optimization of a 5-bar parallel manipulator and the Stewart platform that maximizes the global isotropy index within a predefined workspace. However, kinematic optimization procedure for the isotropy of the antagonistic stiffness in a given workspace has not been applied yet.

As the first step of the optimization procedure, the ISW is defined with respect to the initial kinematic parameters of the mechanism. Then, several steps are conducted to check the existence of the inverse kinematics solution and the stiffness singularity to maximize the optimization index. The optimization procedure is described in Fig.2.

First, position and orientation of the objective ISW are determined to be located within the workspace by initial kinematic parameters. If the predefined ISW cannot be located in the entire workspace calculated, the kinematic parameters of the mechanism should be modified.

Then, the existence of the inverse kinematics solution for the kinematic parameters at the corner of the ISW boundary is checked. The computational verification for kinematic singularity and stiffness singularity is conducted only in the predefined checkpoints in the workspace. After checking the corners, other checkpoints on the boundary of the ISW between the corners are validated whether inverse kinematic solutions exist for all checkpoints. The existence of stiffness singularity for the checkpoints inside the ISW is checked then. The denser sample point will be helpful to check the singularity region.

Finally, these procedures are repeated for various kinematic parameters such as kinematic configuration, link lengths, and positions of the joints of the given mechanism until the optimal kinematic parameters are obtained. The entire workspace and stiffness map for the selected kinematic parameters can be obtained and be optimized.

The proposed optimization procedure has its advantages such as maximizing stiffness properties, ensuring the geometric shape of the ISW and computational efficiency.

III. Formulation of the Optimization Index

A number of criteria have been proposed to represent the property of the stiffness matrix. Xi *et al.* [14] performed a compliant analysis of a tripod-based parallel manipulator. They computed the average and deviation of the trace of a compliance matrix that extended over the entire workspace and discussed dominant factors that affected compliance of the manipulator through compliance mapping. Majou et al. [22] showed the quantitative and qualitative relationship between kinematic parameters and the elements of a stiffness matrix of a 3-DOF translational parallel manipulator (Orthoglide). Xu and Li [23] also investigated the stiffness of a 3-DOF translational parallel manipulator using the screw theory and discussed the influences of the change in kinematic parameters on the stiffness of the manipulator. In their study, several indexes related to the stiffness matrix were compared, and the elements of the stiffness matrix were used as a performance index. However, qualitative comparison of stiffness expressed as the isotropy of the stiffness matrix was not considered.

The performance of parallel manipulators in terms of wrench capability analysis has been conducted in other previous works. Garg *et al.* [24] studied the maximum applicable force and associated moment of the 3-RRRS redundantly actuated parallel mechanism in various positions. Nokleby *et al.* [25] improved the force capability in redundant actuation using the scaling factor method. They used maximum and minimum values of the performance index. In this study, the minimum magnitude of the determinant and the minimum inverse of the condition number of the stiffness matrix are computed to propose the minimum bounds on the stiffness properties produced by the manipulator of optimal kinematic parameters.

In this study, the determinant and the inverse of the condition number of a stiffness matrix are used as performance indexes. The determinant of a stiffness matrix indicates the area of a stiffness ellipse and the inverse of the condition number of a stiffness matrix indicates the isotropy of a stiffness ellipse. Their physical meanings are shown in Fig. 3. A two-by-two stiffness matrix of the 2-DOF parallel manipulator is shown in (1) with its determinant and isotropy presented in (2).

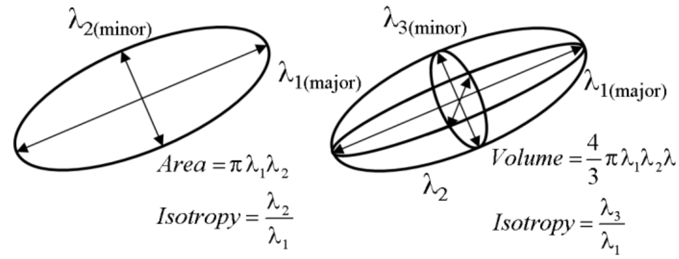

Fig. 3. Eigenvalues of the stiffness ellipse (left) and ellipsoid (right)

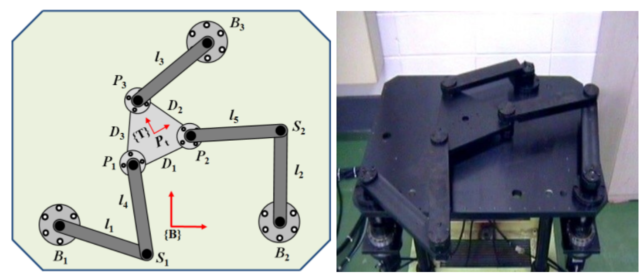

Fig. 4. Schematic diagram of the 2-DOF planar parallel manipulator

TABLE I
Simulation Conditions

Torsion bar	Aluminum (k_1: 216878, k_2: 231919, k_3: 227981) Nmm/rad
Kinematic parameter	l_1, l_2, l_3, l_4, l_5
Working mode	Eight mechanism configurations
ISW shape	Rectangular
ISW area	182 mm (w) * 110 mm (h)

TABLE II
Simulation Results

Original kinematic parameter settings					
Minimum isotropy of stiffness					0.1848
Minimum determinant of stiffness					20.0661
Average isotropy of stiffness					0.4304
Average determinant of stiffness					119.0675
ISW to total workspace ratio (%)					18.2
Parameter setting (mm)	l_1 280	l_2 280	l_3 280	l_4 280	l_5 280
Optimal kinematic parameter settings					
Minimum isotropy of stiffness					0.3183(72.2%)
Minimum determinant of stiffness					108.0390(438.4%)
Average isotropy of stiffness					0.5131(19.2%)
Average determinant of stiffness					146.6552(23.2%)
ISW to total workspace ratio (%)					27.4(50.5%)
Parameter setting (mm)	l_1 300	l_2 300	l_3 200	l_4 370	l_5 370

$$K = K_{active} + K_{passive} = \begin{bmatrix} k_{a11} & k_{a12} \\ k_{a21} & k_{a22} \end{bmatrix} + \begin{bmatrix} k_{p11} & k_{p12} \\ k_{p21} & k_{p22} \end{bmatrix} = \begin{bmatrix} a & b \\ c & d \end{bmatrix} \quad (1)$$

$$det(K) = (ad - bc)$$

$$cond(K) = \frac{\lambda_{\max}}{\lambda_{\min}} = \frac{(a+d)+\sqrt{((a+d)^2 - 4(ad-bc))}}{(a+d)-\sqrt{((a+d)^2 - 4(ad-bc))}}. \quad (2)$$

The optimization index that contains the determinant and the isotropy of the stiffness matrix multiplied by weight factor ω can be expressed as follows:

$$I_S(L) = \max_{L\,[\Psi=\Psi(L_i, i=1\sim N)]} \left[\omega \left(\frac{\min_{i=1\sim n} \det(K_i(\Psi,\tau_r))}{\min_{i=1\sim n} \det(K_{oi}(\Psi,\tau_r))} \right) + (1-\omega) \left(\frac{\min_{i=1\sim n} 1/cond(K_i(\Psi,\tau_r))}{\min_{i=1\sim n} 1/cond(K_{oi}(\Psi,\tau_r))} \right) \right]$$

$$\text{subject to ISW} \quad (3)$$

Each term of (3) is divided by the values of the original manipulator, to takes a dimensionless form and to compare the performance from the original kinematic parameter setting. The minimum value is considered to be a performance index because it shows that the manipulator can guarantee the minimum value in all checkpoints of the ISW.

IV. Case Study (2-DOF Planar Type Parallel Manipulator)

In this section, a 2-DOF planar parallel manipulator is introduced and the kinematic parameters are optimized by applying the optimization procedure. The manipulator consists of five links l_{ij} and a tool plate [2]. This manipulator also has eight revolute joints: three ground joints denoted by B_i, two intermediate joints S_i, and three tool plate joints P. The manipulator has two kinematic degrees of freedom and three actuated joints [26]. Although it contains x, y-translational and z-rotational motions, the rotational motion is determined by x, y-translational motion, so it has only 2-DOF. The schematic diagram of the 2-DOF planar parallel manipulator is shown in Fig. 5.

The simulation results are presented in two cases. The first simulation is related to the original kinematic parameter settings and the second simulation related to the optimal kinematic parameter settings, respectively. The detailed simulation condition is presented in Table I. In total, eight mechanism configurations can be generated from eight combinations of the inverse kinematic solutions. The objective ISW area was obtained as 182 mm (w) * 110 mm (h) which is the maximum area that can be obtained from the original kinematic parameter settings.

In Fig. 5 and Fig. 6, the left upper graph shows the inverse of the condition number of constraint Jacobian (kinematic singularity measure) in the non-redundant case, the right upper graph shows the inverse of the condition number in the redundant case, the left lower graph shows the inverse of the condition number of the stiffness matrix (isotropy of stiffness),

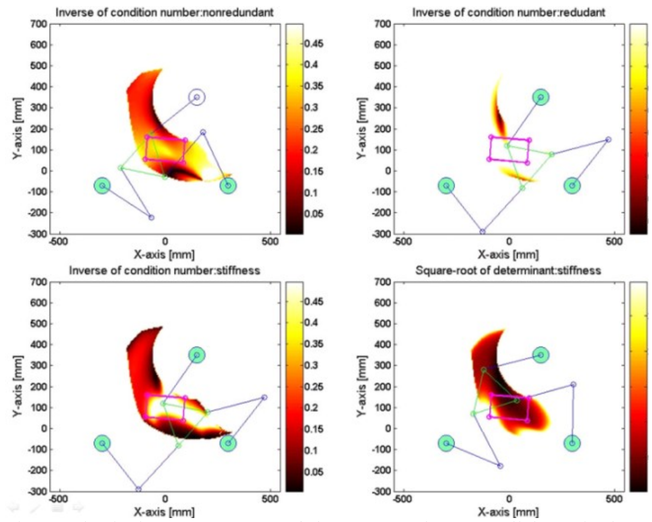

Fig. 5. Physical property maps of the 2-DOF planar parallel manipulator with the original kinematic parameter settings

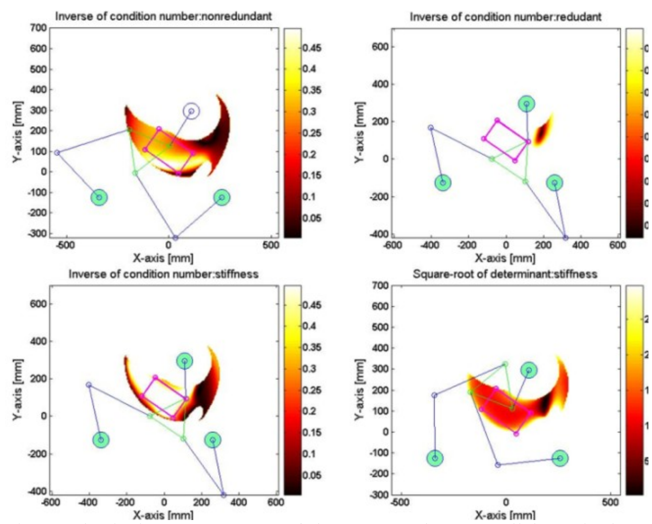

Fig. 6. Physical property maps of the 2-DOF planar parallel manipulator with the optimal kinematic parameter settings

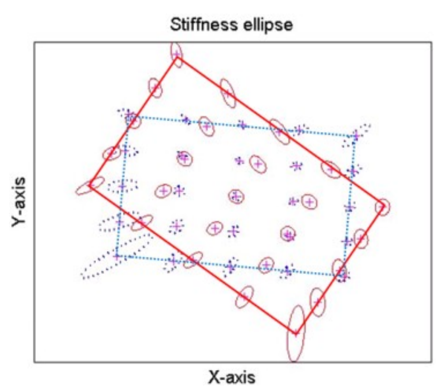

Fig. 7. Change of stiffness ellipses of 25 checkpoints (dotted line: before, solid line: after)

and the right lower graph shows the determinant of the stiffness matrix (magnitude of stiffness). The upper two graphs of each case show that the redundant mechanism has increased the inverse of the condition number in each simulation case. The rectangular shaped ISWs were drawn in all graphs.

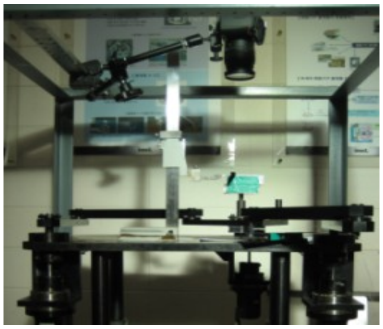

(a) Measurement setup

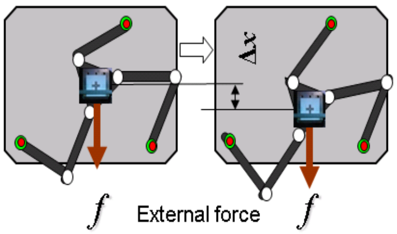

(b) External force and displacement

Fig. 8. Experimental setup to measure the displacement of end-effector

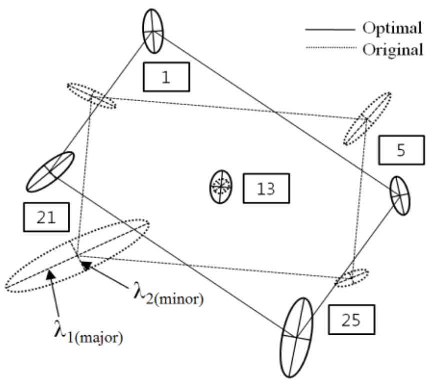

Fig. 9. Comparison of five stiffness ellipse pairs measured by the experiment

The simulation results are also shown in Table II. Comparing the two simulation cases, the enlarged ISW area was obtained in spite of showing relatively high isotropy of stiffness. Moreover, the minimum isotropy generated inside of the ISW was increased to 72.2%. In addition, there was a rapid change of magnitude of stiffness in the original case, whereas this property showed more uniform distribution in the optimal case. The high ISW-to-total-workspace ratio (50.5%) represents an increase in efficiency of the workspace utility. The ISW located inside the workspace and the stiffness properties of the optimization result are shown in Fig. 7. There are four vertexes and one center checkpoint. Figure 7 indicates two ISWs and the displacement graphs of the original case and the optimal case of the 2-DOF planar parallel manipulator, respectively. In addition, the optimal result in Fig. 7 shows the enlarged ISW and decreased displacement graph when compared to the original one with stiffness ellipses of 25 checkpoints within each setting of ISW. Through the simulation results, it is ascertained that the optimization improves both the ISW area and stiffness property of the 2-DOF planar parallel manipulator

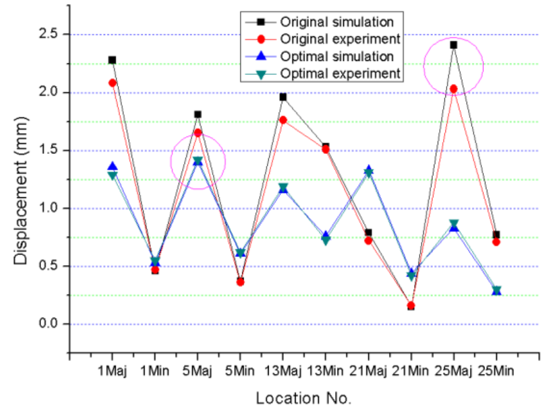

Fig. 10. Displacements along the major and the minor axes of the five experimental locations

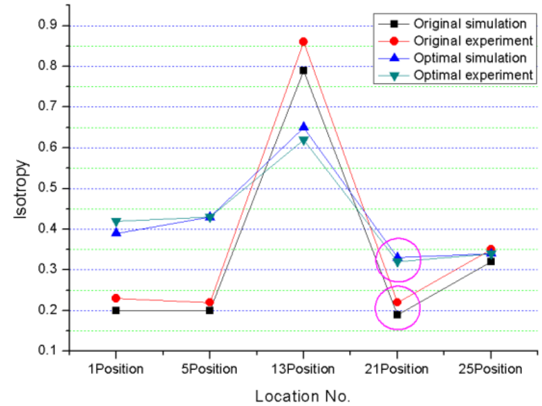

Fig. 11. Isotropy of stiffness of the five experimental locations

simultaneously.

A noncontact measurement method is required to measure the displacement of the end-effector of the 2-DOF planar parallel manipulator, because the measured displacement can be changed by an external force exerted on the end-effector. The optical measurement method using high resolution camera is applied to satisfy the requirement above. The experimental setup is depicted in Fig. 8. Stepwise external forces are applied along the major and minor directions by imposing force through steel string and induced displacements are measured by the camera mounted in vertical direction to the tool plate. The method takes pixel data of the end-effector position/orientation and transforms the pixel data into coordinate data. The coordinate data is obtained from three repeated measurement of the displacement.

The measured data corresponds to the major and minor axes of the stiffness ellipse at five checkpoints located in the ISW in forward/backward directions. In Fig. 9 comparison of five experimental stiffness pairs of the original and optimal cases are depicted. The overall stiffness properties of five locations were improved. Exact measured data are shown in Fig. 10 and Fig. 11. Each figure represents displacement and isotropy of stiffness, respectively. In the figures, circular and inverted triangular marks are related to the experimental results while rectangular and triangular marks relate to the simulation results. The experiment results show the validity of the stiffness analysis and the improvement of stiffness obtained from the optimization procedure. In most cases, the measured displacements decreased compared to the simulation ones. The decrease seems to be caused by friction effect existing between connection parts of each link of the 2-DOF planar parallel manipulator. In the overall experimental data, the magnitude and isotropy of the stiffness of the optimal case are larger than in the original case. The isotropy and magnitude of stiffness found in the five checkpoints improved in the optimal original cases by 31.7% and 45.5%, respectively.

The two experimental results show that the stiffness analysis that starts from the virtual work theorem under the assumption of quasi-static motion is reasonable. The manipulator with a new kinematic parameter set shows higher stiffness properties compared to the original manipulator in terms of isotropy and magnitude.

V. Conclusion

An optimization procedure was developed and applied to maximize stiffness properties within the isotopic stiffness workspace and to ensure the workspace shape for a redundantly actuated parallel manipulator. A new optimization index was formulated based on the antagonistic stiffness modeling, which takes into account the magnitude and the isotropy of the stiffness matrix. An optimal kinematic parameter set of a 2-DOF planar parallel manipulator was calculated by the suggested optimization procedure. The inverse of the condition number and the determinant of the stiffness matrix were observed to have higher values than the values from the original kinematic parameter set. Displacement of the end-effector of the 2-DOF parallel manipulator under external force was measured by optical measurement system. The experimental data supported the improvement in the stiffness properties. The result demonstrates the validity of the method in finding optimal kinematic parameter that satisfy the shape of the ISW and increase the stiffness properties within the workspace.

As future works, the consideration of global optimization using design of experiments and analytical optimization process will be valuable. Moreover, the more DOFs stiffness enhancement could be considered especially when the rotational stiffness and translational stiffness should be taken into account together. The influence of the optimization parameters such as weight value ω and number of check points n will also be considered.

References

[1] J. Kim, J.-. Hwang, J.-S. Kim, C. C. Iurascu, F.C. Park and Y. M. Cho, “Eclipse-II: A New Parallel Mechanism Enabling Continuous 360-degree Spinning Plus Three-axis Translational Motions,” *IEEE Transactions on Robotics and Automation*, vol.18, no.3, pp.367 -373, 2002.

[2] S. Kim, W. In, H. Yim, J. I. Jeong, F. C. Park, and J. Kim “Stiffness enhancement of a redundantly actuated parallel manipulator using internal preload: Application to a 2-d.o.f parallel mechanism,” in *Asian Symposium for Precision Engineering and Nanotechnology*, 2007.

[3] A. Müller, “Internal Preload Control of Redundantly Actuated Parallel Manipulator - Its Application to Backlash Avoiding Control,” *IEEE Transactions on Robotics and Automation*, Vol. 21, pp. 668-677, 2005.

[4] S.-H. Hyon, "A Motor Control Strategy With Virtual Musculoskeletal Systems for Compliant Anthropomorphic Robots," *IEEE/ASME Transactions on Mechatronics*, vol. 14, no. 6, pp.677-688, 2009.

[5] B.-S. Kim, J.-B. Song, and J.-J. Park, "A Serial-Type Dual Actuator Unit With Planetary Gear Train: Basic Design and Applications", *IEEE/ASME Transactions on Mechatronics*, vol. 15, no. 1, pp.108-116, 2010.

[6] X.-J. Liu, J. Wang, and G. Pritschow, “Performance atlases and optimum design of planar 5R symmetrical parallel mechanisms,” *Mechanism and Machine Theoy* , vol. 41, pp.119-144, 2006.

[7] X.-J. Liu, J. Wang, and G. Pritschow, “Kinematics, singularity and workspace of planar 5R symmetrical parallel mechanisms,” *Mechanism and Machine Theory*, vol.41, pp.145–169, 2006.

[8] A. Kosinska, M. Galicki and K. Kedzior, “Determination of parameters of 3-dof spatial orientation manipulators for a specified workspace,” *Robotica*, Vol.20, pp. 179–183, 2002.

[9] M. Ceccarelli, and C. Lanni, “A multi-objective optimum design of general 3R manipulators for prescribed workspace limits,” *Mechanism and Machine Theory*, vol.39, pp.119–132, 2004.

[10] G. Carbone, and M. Ceccarelli, “Comparison of indices for stiffness performance evaluation,” *Front. Mech. Eng. China*, vol. 5, no. 3, pp. 270–278, 2010.

[11] J. H. Lee, B.-J. Yi, S.-R. Oh, and I. H. Suh, “Optimal Design of a Five-bar Finger with Redundant Actuation,” in *Proceedings of the 1998 IEEE International Conference on Robotics & Automation*, Leuven, 1998.

[12] R. Kurtz and V. Hayward, “Multiple-Goal Kinematic Optimization of a Parallel Spherical Mechanism with Actuator Redundancy,” *IEEE Transactions on Robotics and Automation*, vol. 8, no. 5, 1992.

[13] D. Chakarov, “Study of the Antagonistic Stiffness of Parallel Manipulators with Actuation Redundancy,” *Mechanism and Machine Theory*, vol. 39, pp.583-601, 2004.

[14] J. Kim, F. C. Park, S. J. Ryu, J. Kim, J. Hwang, C. Park, and C. Iurascu, “Design and analysis of a Redundantly Actuated Parallel Mechanism for Rapid Machining,” *IEEE Transactions on Robotics and Automation*, vol.17, no.4, pp.423 -434, 2001.

[15] L. Wang, J. Wu, J. Wang, and Z. You, "An Experimental Study of a Redundantly Actuated Parallel Manipulator for a 5-DOF Hybrid Machine Tool," *IEEE/ASME Transactions on Mechatronics*, vol.14, no.1, pp.72-81, 2009.

[16] T. Huang, Z. Li, M. Li, D. G. Chetwynd, and C. M. Gosselin, “Conceptual Design and Dimensional Synthesis of a Novel 2-DOF Translational Parallel Robot for Pick-and-Place Operations,” *Journal of Mechanical Design*, vol. 126, pp.449-455, 2004.

[17] C. Gosselin, and J. Angeles, “Singularity Analysis of Closed-Loop Kinematic Chains,” *IEEE Transactions on Robotics and Automation,* vol. 6, pp. 281-290, 1990.

[18] F.C. Park, and J.W. Kim, “Singularity Analysis of Closed Kinematic Chain,” *ASME Journal of Mechanical Design*, vol. 121, no. 1, pp. 32-38, 1999.

[19] E. Lee, C. Mavroidis, and J. P. Merlet, “Five Precision Point Synthesis of Spatial RRR Manipulators Using Interval Analysis,” *Journal of Mechanical Design*, vol. 126, pp.842-849, 2004.

[20] A. P. Morgan, and C. W. Wampler, “Solving a Planar Four-Bar Design Problem Using Continuation,” *Journal of Mechanical Design*, vol. 112, pp.544-550, 1990.

[21] L. Stocco, S. E. Salcudean and F. Sassani, “Fast constrained global minimax optimization of robot parameters,” *Robotica*, vol. 16, pp. 595–605, 1998.

[22] F. Majou, C. Gosselin, P. Wenger, and D. Chablat, “Parametric stiffness analysis of the Orthoglide,” *Mechanism and Machine Theory,* vol. 42, pp. 296–311, 2007.

[23] Q. Xu and Y. Li, "An investigation on mobility and stiffness of a 3-DOF translational parallel manipulator via screw theory," *Robotics and Computer Integrated Manufacturing*, vol. 24, no. 3, pp.402-414, 2008.

[24] V. Garg, S. B. Nokleby, and J. A. Carretero, “Wrench capability analysis of redundantly actuated spatial parallel manipulators,” *Mechanism and Machine Theory* , vol. 44, pp.1070-1081, 2009.

[25] S. B. Nokleby, R. Fisher, R. P. Podhorodeski, and F. Firmani, “Force capabilities of redundantly-actuated parallel manipulators,” *Mechanism and Machine Theory*, vol. 40, pp.578-599. 2005.

[26] J. I. Jeong, D. Kang, Y. M. Cho, and J. W. Kim, “Kinematic calibration for redundantly actuated parallel mechanisms,” *Journal of Mechanical Design*, vol. 126, pp.307-318, 2004.